Design and Validation of a Driver Guidance System to Alleviate Passenger Motion Sickness

Weiyin Xie[a,c], Haolong Hu[b], Dengbo He[a,b,*]

[a] Thrust of Robotics and Autonomous Systems, The Hong Kong University of Science and Technology (Guangzhou), Guangzhou, China

[b] Thrust of Intelligent Transportation, The Hong Kong University of Science and Technology (Guangzhou), Guangzhou, China

[c] School of Digital Media and Interactive Design, Guangzhou Maritime University, Guangzhou, China

[*]Corresponding author. Email: dengbohe@ust.hk

ABSTRACT

Motion sickness (MS) remains a major issue in smart cabins, especially when passengers conduct non-driving-related tasks. Previous research mostly addressed this issue from the passenger's perspective, for example, by providing interfaces informing the motion state of the vehicle. However, as a major source of MS, the driver's behaviors were rarely regulated, though it is well-acknowledged that aggressive driving style can lead to more severe MS. Thus, as a first attempt, we proposed an interactive driver guidance system aiming at reducing MS among passengers, which provided drivers real-time information on the vehicle acceleration, and visual alerts regarding potentially MS-inducing maneuvers. In an on-road experiment with a within-subjects design, 16 gender-balanced driver–passenger pairs (32 participants in total) completed a 30-minute urban route driving task, under two conditions (with and without the guidance system) to validate the system. Passengers reported their MS levels at a one-minute interval, using the Misery Scale (MISC). The results show that while no significant differences were found in overall driving distance or Motion Sickness Dose Value, our guidance system led to lower levels of acceleration over time. Correspondingly, we observed a lower likelihood of passengers experiencing mild ($MISC \geq 2$) or higher MS when drivers were provided with the guidance system, compared to when such a system was absent. These findings suggest that the system effectively facilitated MS-friendly driving styles and delayed the onset of MS among passengers. Our study demonstrates the potential of driver guidance systems to improve ride comfort, especially during ridesharing and short-distance travel.

Keywords: motion sickness; driver behavior guidance; on-road study; smart cabin

1. Introduction

With the rapid advancement of automotive technology, the smart cabin that integrates advanced driver assistance, infotainment, and personalized services has become increasingly vital to modern vehicles (Aarti, 2025). By incorporating sensors, real-time data processing, and interactive displays, smart cabins aim to enhance the in-car experience for both drivers and passengers. While these innovations improve comfort and efficiency, they also introduce new challenges, particularly motion sickness (MS), which remains a main barrier to the widespread acceptance of smart cabins. The MS manifests in symptoms such as dizziness, nausea, and, in severe cases, vomiting (Smyth, Birrell, et al., 2021; Smyth, Robinson, et al., 2021). These symptoms are often exacerbated by aggressive driving behaviors (Brietzke et al., 2021) and large or abrupt accelerations (Irmak et al., 2022).

Previous research regarding MS mitigation among passengers primarily focused on providing additional visual (Li et al., 2024) or auditory cues (Maculewicz et al., 2021) to support the anticipation or perception of vehicle movements. While such interventions often work, they do not directly address the primary source of motion disturbances, i.e., the control of the vehicle. For vehicles with driving automation, the optimization of vehicle path planning or suspension control has been found to alleviate MS (DiZio et al., 2018; Siddiqi et al., 2022). However, before driving automation saturates the market, drivers still need to control the vehicle most of the time.

Previous studies have found that driving style was associated with the chance of MS among passengers, with a defensive driving style significantly leading to less discomfort than an aggressive driving style (Brietzke et al., 2021; Karjanto et al., 2022). The driving style, though related to drivers' own personality, can be affected by real-time in-vehicle feedback systems (Vaezipour et al., 2015). However, to date, although the in-vehicle feedback systems have been designed to improve the fuel efficiency (e.g., speed feedback by Barth and Boriboonsomsin (2009)) and driving safety (e.g., real-time advice providing by Vaezipour et al. (2018)) in previous research, to the best of

our knowledge, no such system has been designed to mitigate MS, particularly in the context of modern smart cabins, which is able to provide interactive feedback to drivers.

To address this gap, the present study proposes an in-vehicle, screen-based guidance system to promote MS-friendly driving behaviors. This system evaluates driving behavior concerning passenger MS and provides real-time feedback on acceleration patterns and the potential risk of MS, alerting drivers of maneuvers that may induce or exacerbate passenger MS. Unlike passenger-focused solutions (e.g., providing vehicle motion cues to passengers), our proposed system targets the underlying cause of MS in human-driven vehicles. Through a combination of human-machine interface (HMI) design, real-world testing, and MS assessments, this study aims to examine how visual driver feedback influences MS-related driving behaviors and evaluate its impact on passenger MS. An on-road within-subject design experiment was conducted, where drivers alternated between conditions with and without the guidance system. We propose the following hypotheses for our study:

- **H1:** With the driver guidance system, the driving style will be more conservative, and the vehicle dynamics will be smoother than when the system is absent.
- **H2:** With the driver guidance system, passengers will experience less MS than when the system is absent.

2. Background

2.1. Theories Explaining the Occurrence of MS

MS has been extensively studied from the perspective of human motion perception and sensory integration. One of the most widely adopted explanations is the sensory conflict theory, which attributes MS to mismatches among vestibular signals, visual input, and somatosensory motion cues (Reason, 1975). According to this theory, MS arises when these sensory systems provide conflicting information about movement. For example, a passenger watching a video in a moving vehicle perceives a relatively static environment inside the cabin, and the somatosensory cues also indicate the

absence of body movement. However, the vestibular system still detects the vehicle's acceleration relative to the road. This sensory mismatch can trigger MS. Building on the sensory conflict framework, the subjective vertical conflict theory has also been applied to explain MS by emphasizing the role of perceived upright orientation in sensory integration (Bos & Bles, 1998). This theory suggests that MS occurs when discrepancies arise between the internal perception of verticality (subjective vertical) and the actual gravitational vertical. Such conflicts can result from disturbances in vestibular, visual, and proprioceptive inputs, particularly in dynamic environments where the expected and perceived vertical orientations do not align.

In addition to sensory-conflict-based explanations, an alternative theoretical account is the postural instability theory, which posits that MS emerges when individuals are unable to maintain stable control of posture over time, rather than from conflicts among sensory signals (Riccio & Stoffregen, 1991). Taken together, these theoretical perspectives converge on the influence of vehicle motion on MS risk, albeit through different explanatory pathways, as vehicle dynamics directly influence sensory integration, perceived verticality, and postural control demands.

2.2. Driving Style as a Determinant of MS

A substantial body of empirical research has investigated how driving styles in automated vehicles influence passenger comfort and MS. In this line of work, vehicle motion characteristics such as longitudinal acceleration and deceleration profiles, braking smoothness, and cornering dynamics have been shown to play a critical role in shaping passenger experience. Studies on automated driving consistently report that smoother acceleration, gentler braking, and more gradual cornering trajectories are associated with improved ride comfort and reduced MS and thus can be identified as MS-friendly driving style, whereas abrupt or high-magnitude maneuvers tend to exacerbate discomfort and MS symptoms (e.g., De Winkel et al., 2023; Htike et al., 2020; Paganelli et al., 2022; Siddiqi et al., 2022).

Although these findings are often derived from automated driving contexts, the underlying mechanisms are fundamentally linked to vehicle dynamics rather than the source of vehicle control. This suggests that the relationship between driving style and MS is not exclusive to automated vehicles, but should also apply to manually driven scenarios in which a human driver determines acceleration, braking, and steering.

Consistent with this view, studies focusing on human driving behavior have shown that aggressive driving styles, characterized by larger longitudinal and lateral accelerations, can lead to more severe MS compared to conservative driving styles, particularly when passengers engage in non-driving-related tasks (Karjanto et al., 2022; Vaiana et al., 2014). One key contributing factor is acceleration amplitude: experimental work has demonstrated that MS severity increases with a stronger dynamic stimulation (Irmak et al., 2022), and that higher dynamic intensity in stop-and-go traffic is associated with increased MS (Brietzke et al., 2021). Beyond MS, higher acceleration levels have also been linked to reduced subjective comfort ratings (De Winkel et al., 2023).

2.2. Quantifying MS and Vehicle Dynamics

MS, as a subjective experience, varies among individuals. However, the likelihood of having MS can still be estimated through mathematical models. One such model is the Motion Sickness Dose Value (MSDV) (Donohew & Griffin, 2004; ISO2631-1, 1997), which quantifies MS induced by vehicle dynamics by integrating acceleration over time. Turner and Griffin (1999) found strong correlations between MSDV and passenger MS in buses, with $R^2 = 0.77$ for lateral MSDV and $R^2 = 0.79$ for longitudinal MSDV.

Building on the subjective vertical conflict theory (Bos & Bles, 1998), Kamiji et al. (2007) further introduced a 6-degree-of-freedom (DoF) subjective vertical conflict (SVC) model to quantify sensory conflict. This model estimates MS incidence (MSI), i.e., the percentage of individuals expected to experience MS under specific head motion stimuli, using inputs such as head acceleration, head angular velocity, and

gravitational forces in a head-fixed coordinate system. Previous studies have demonstrated a good match between MSI value and actual likelihood of observing MS (Wada & Yoshida, 2016). To further improve the practicability of MSI, Buchheit et al. (2021) adapted this model to estimate MS using only vehicle dynamics data by mapping vehicle motion to head dynamics through a simplified human-vehicle model.

2.3. Existing Approaches to MS Alleviation

Most existing approaches to MS alleviation focus on passenger-oriented interventions, particularly through the provision of motion cues that represent current or upcoming vehicle movements. Such cues aim to improve passengers' ability to perceive and anticipate vehicle motion, thereby reducing sensory conflict. Examples include visual representations of vehicle motion on mobile displays (Li et al., 2024), embedding live road videos into reading interfaces (Miksch et al., 2016), and using interior LED strips to signal upcoming vehicle maneuvers in automated vehicles (Karjanto et al., 2018). While these approaches have shown promise, they primarily target passengers rather than the underlying cause of MS, namely, vehicle dynamics shaped by driving behavior. Moreover, passenger-oriented cues may interfere with NDRTs and reduce task engagement or comfort.

2.4. Research Gap: Driver Guidance via In-Vehicle HMI

An alternative strategy is to directly influence driving behavior. Prior research has shown that driving behavior can be improved through active in-vehicle feedback systems (Vaezipour et al., 2015). For instance, a simulator study by Vaezipour et al. (2018) has demonstrated the effectiveness of these systems in promoting eco-safe driving by providing real-time advice and feedback to drivers, encouraging them to adopt a style that can lower fuel consumption and enhance safety. Similarly, Barth and Boriboonsomsin (2009) found that speed feedback via in-vehicle dashboard displays can reduce fuel consumption by 10-20%, depending on the context of the driving scenario. In a related line of work, a study by Xu et al. (2023) on speed limit advisory

systems has shown that recommending reduced speeds for hazardous road sections can significantly improve driver safety. However, despite extensive work on MS-friendly driving style of driving automation and passenger-oriented MS mitigation strategies, it remains unclear whether in-vehicle HMI-based guidance can be used to coach a human driver toward a MS-friendly driving style while retaining manual control. Addressing this gap is the primary focus of the present study.

3. Methodology

3.1. Participants

A total of 32 participants were recruited through online forums and campus posters, acting as drivers (n = 16) and passengers (n = 16). These participants were grouped into 16 fixed pairs, each consisting of one driver and one passenger. The pairs remained consistent across all trials. Passenger participants (8 males and 8 females) had a mean age of 24.3 years (range: 19 – 36; standard deviation [SD] = 5.8). We intentionally recruited passengers participants with higher susceptibility to MS, as they may suffer more in inappropriately designed cabins and were more likely to benefit from our proposed countermeasures. Thus, all passenger participants were required to score above the 75th percentile on the Motion Sickness Susceptibility Questionnaire Short-form (MSSQ-short, Golding (2006); Li et al. (2023)), i.e., a minimum score of 19 out of 54. As the study was conducted in mainland China, a validated Chinese version of the MSSQ-Short was used (Lin & Guo, 2022). As a result, the average MSSQ-short score among passengers was 23.4 (range: 19–43.2; standard deviation [SD] = 6.5). Besides, all participants self-reported good overall health and normal vestibular function.

Driver participants (8 males and 8 females; mean age = 28.3 years, SD = 5.5, range: 22–41) were recruited based on their driving style, focusing on those exhibiting aggressive tendencies. Driving style was assessed using the Chinese version of the Multidimensional Driving Style Inventory (MSDI-C; Sun et al., 2014), which includes

five factors that form three distinct driving styles. This study specifically focused on the risky driving style, characterized by high speeds and aggressive behavior, which is measured by the *risky* and *sensation-seeking* subscales. The average risky driving score among participants was 3.0 (SD = 0.6; range: 2.3–4.3), with a mean sensation-seeking score of 1.9 (SD = 0.8; range: 1–4). To ensure the safety of the on-road study, all drivers had no history of moderate or severe traffic accidents in the past five years, had at least two years of driving experience, and reported an annual driving distance of at least 5,000 kilometers.

3.2. Equipment

As illustrated in Figure 1, a fuel-powered Volkswagen Magotan was used for the experiment. An IM948 Inertial Measurement Unit (IMU) was mounted on the horizontal surface of the glove compartment in the center of the front row (see Fig. 1). The IMU recorded linear acceleration data at a sampling rate of 30 Hz with a precision of 0.01 G. The coordinate system adhered to the right-hand convention as defined in ISO8855 (2011), with the z-axis pointing upward (vertical), the x-axis pointing forward (longitudinal), and the y-axis pointing to the right (lateral) of the vehicle.

A custom software program running on an onboard laptop processed the real-time acceleration and orientation data from the IMU to evaluate driving behavior from the perspective of MS. Based on this evaluation, an appropriate feedback interface was generated and displayed to the driver on a 7-inch screen, which was mounted to the right side of the steering using a holder attached to the dashboard (see Fig. 1).

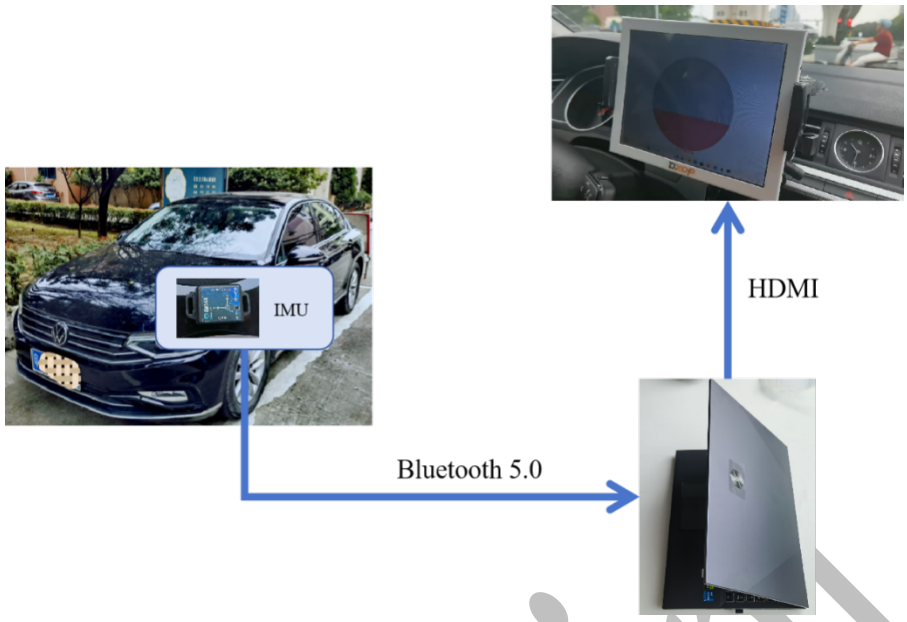

Figure 1. Equipment used for generating real-time feedback for drivers.

To simulate typical rear-seat entertainment display setups in commercial vehicles, a 9.7-inch iPad was securely mounted on the back of the front passenger seat (see Fig. 2). This in-vehicle display played video content throughout the ride, serving as an experiment task for the passenger. A mounting bracket was used to ensure the screen's position and orientation remained consistent across all trials.

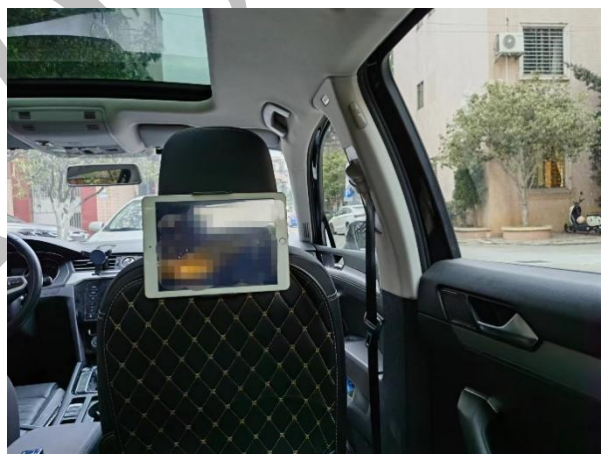

Figure 2. Position of the in-vehicle entertainment display for passengers.

3.3. Driver Guidance System Design

Three interfaces were designed in our driver guidance system, with their key parameters decided using a Six-Degrees-of-Freedom Subjective Vertical Conflict (6-DoF SVC) model by Buchheit et al. (2021). Thus, in this section, we will first introduce the 6-DoF SVC model and then provide details of the interface design.

3.3.1 The 6-DoF SVC Model

For the calculation of the 6-DoF SVC, vehicle dynamics data was first transformed into head dynamics using a simplified human-vehicle model. Then, the head dynamics were input into the 6-DoF SVC model to compute the MSI.

In the simplified human-vehicle model, it was assumed that the passenger's body exhibits no damping effect. The coordinate origin of the head reference frame was relocated to the center of gravity of the vehicle, and the rotational acceleration resulting from vehicle movement was neglected. Based on these assumptions, the head dynamics, which served as the input to the 6-DoF SVC model, were calculated as follows (from equations (1) to (8)):

$$\dot{\boldsymbol{\omega}}_{\boldsymbol{head}}(\boldsymbol{t}) = \frac{d}{dt}\omega_{head}(t) \quad (1)$$

$$\boldsymbol{a}_{\boldsymbol{head}}(\boldsymbol{t}) = \boldsymbol{M}_{\boldsymbol{rot}}((\boldsymbol{\omega}_{\boldsymbol{head}}(\boldsymbol{t})^{\boldsymbol{T}}))\boldsymbol{a}_{\boldsymbol{car}}(\boldsymbol{t}) \quad (2)$$

$$f_{head}(t) = M_{rot}((\boldsymbol{\omega}_{\boldsymbol{head}}(\boldsymbol{t}))^{T})g + a_{head}(t) \quad (3)$$

Where:

$$\boldsymbol{\omega}_{\boldsymbol{head}}(\boldsymbol{t}) = \boldsymbol{M}_{\boldsymbol{rot}}(\Phi_{\boldsymbol{h}}, \boldsymbol{\theta}_{\boldsymbol{h}}, \boldsymbol{\Psi}_{\boldsymbol{h}}) \cdot \left(\boldsymbol{f}_{\boldsymbol{h}} \circ \boldsymbol{\omega}_{\boldsymbol{car}}(\boldsymbol{t})\right) \quad (4)$$

$$\boldsymbol{M}_{\boldsymbol{rot}}(\Phi_{\boldsymbol{h}}, \boldsymbol{\theta}_{\boldsymbol{h}}, \boldsymbol{\Psi}_{\boldsymbol{h}}) = M_{roll}(\Phi)M_{pitch}(\Phi)M_{yaw}(\Phi) \quad (5)$$

And:

$$M_{roll}(\Phi) = \begin{bmatrix} 1 & 0 & 0 \\ 0 & \cos(\Phi) & \sin(\Phi) \\ 0 & -\sin(\Phi) & \cos(\Phi) \end{bmatrix} \quad (6)$$

$$M_{pitch}(\boldsymbol{\theta}) = \begin{bmatrix} \cos(\boldsymbol{\theta}) & 0 & -\sin(\boldsymbol{\theta}) \\ 0 & 1 & 0 \\ \sin(\boldsymbol{\theta}) & 0 & \cos(\boldsymbol{\theta}) \end{bmatrix} \quad (7)$$

$$M_{yaw}(\boldsymbol{\Psi}) = \begin{bmatrix} \cos(\boldsymbol{\Psi}) & \sin(\boldsymbol{\Psi}) & 0 \\ -\sin(\boldsymbol{\Psi}) & \cos(\boldsymbol{\Psi}) & 0 \\ 0 & 0 & 1 \end{bmatrix} \quad (8)$$

Additionally, it was assumed that the passenger's body motion was fully synchronized with the vehicle's three-dimensional rotation. We specified the compliant head condition, defined as $f_h = (1, 1, 1)^T$, that which corresponded to a passive passenger whose gaze remained fixed forward, i.e., $(\phi_h, \theta_h, \varphi_h)^T = 0$ and who did not employ any active compensation strategies.

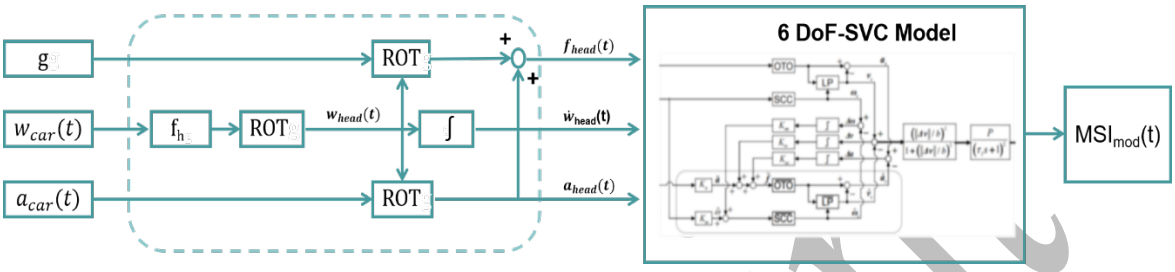

Figure 3. The motion transfer function (Human-Vehicle Model) and the 6-DoF SVC model from Buchheit et al. (2021); Here, ROT denotes the rotation process, *fh* represents the head-movement factor, and *g* is the gravity vector.

The parameters for the 6-DoF-SVC model were also adopted from the study by Buchheit et al. (2021) (see Table 1).

Table 1. Parameter setting by Buchheit et al. (2021)

K_a	K_w	K_{ac}	K_w	K_{vc}
0.1	0.8	0.35	0.8	1
b [m/s^2]	P[%]	T[s]	T_d[s]	T_a[s]
0.1	88	720	7.0	190

Typically, MSI is calculated using the entire set of dynamic data accumulated progressively from the beginning of the ride. However, the increase in MSI is nonlinear with respect to dynamic input, meaning that even with identical motion patterns, the MSI tends to rise more rapidly in the early phase of the ride than in the later stages. Thus, to enable a fairer comparison of driving behavior on a minute-by-minute basis,

we adopted MSI_{min}, calculated using only the dynamic data from the most recent one-minute window.

3.3.2 The Interface Design

We designed three distinct interfaces as part of a driver guidance system, corresponding to different stages of vehicle acceleration (see Figure 5):

The encouragement interface was designed to reinforce current driving behavior when vehicle acceleration was slight (and thus less likely to induce MS), in which the inner circle of the HMI turned green and a message “Excellent driving performance” was presented to the driver (see Figure 4).

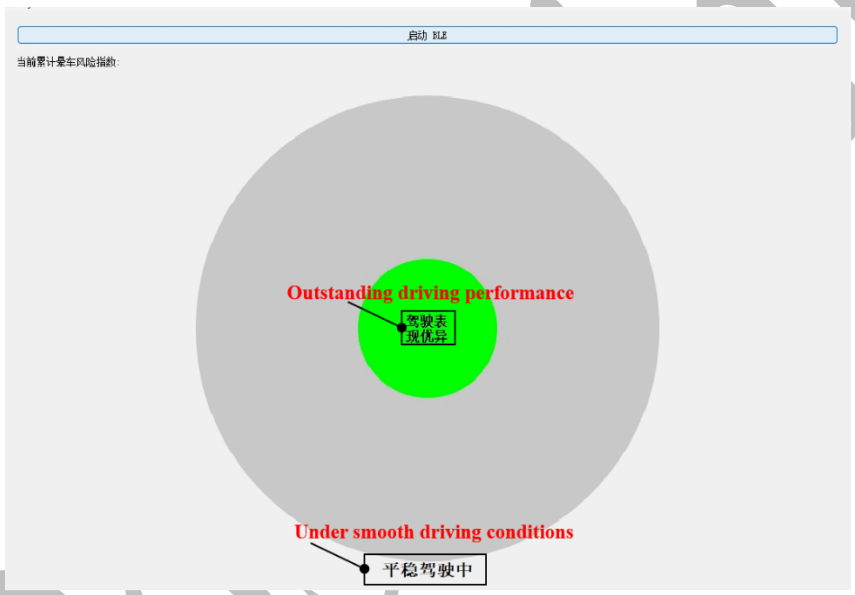

Figure 4. The encouragement interface for encouraging smooth driving.

The warning interface was designed to provide real-time feedback on the current acceleration. Inspired by the concept of a "health bar" commonly used in video games, we introduced an “MS bar”. The bar appears (see Figure 5) when the vehicle's acceleration exceeds an upper acceleration threshold, as defined in Table 2 (De Winkel et al., 2023).

Table 2. Threshold values for different MS risk levels.

Comfort acceleration level in De Winkel et al. (2023)	"Excellent"	"Very good"	"Good"	"So-so"	"Bad"
Acceleration	≤ 0.28m/s^2	≤ 0.56m/s^2	≤ 0.89m/s^2	≤ 1.23m/s^2	≤ 1.89m/s^2
Low risk of MS	lower limit	-	-	-	Upper limit
Medium risk of MS	lower limit	-	-	Upper limit	-
High risk of MS	lower limit	-	Upper limit	-	-

The upper acceleration threshold was dynamically adjusted based on the current MSI level, as estimated by the 6-DoF SVC model. Based on the MSI values, we categorized the MS risk as low (MSI < 5%), medium (5% ≤ MSI < 10%), and high (MSI ≥ 10%). Based on MSI values, MS risk was categorized into three levels: low (MSI < 5%), medium (5% ≤ MSI < 10%), and high (MSI ≥ 10%). Accordingly, the upper acceleration limit was adapted to each risk level: 1.89 m/s² for low risk, 1.23 m/s² for medium risk, and 0.89 m/s² for high risk. When acceleration exceeded the threshold, a red bar began to fill the outer ring of the interface. The more the acceleration surpassed the threshold, the higher the bar became. The ratio of the circle being filled by the bar was defined as follows:

$$ratio = \max\left(\frac{acceleration - upper\ threshold}{upper\ threshold}, 100\%\right)$$

Once the acceleration fell below the upper limit, the MS bar began to recede at a speed of v (see Figure 5), which was defined as follows:

$$v = (1 + \mathrm{MSI}_{min}) * 0.005/s$$

Accordingly, the ratio was updated as follows:

$$ratio = ratio - v * t$$

Where t is the duration of the falling time. Throughout this period, a textual warning was shown, notifying the driver that there was a risk of MS.

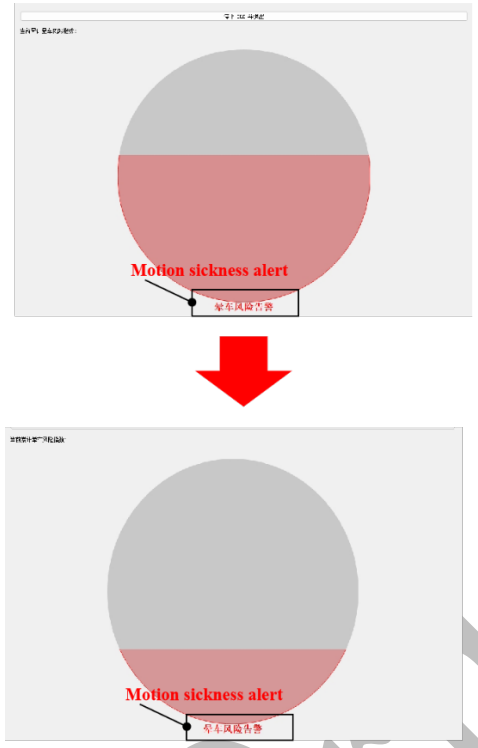

Figure 5. The warning interface to warn of MS-leading driving behaviors.

The informative interface was designed to alert the driver when the acceleration became harsh (and thus may potentially induce MS), in which a red arrow appeared on the outer circle, indicating the direction of the inertial force acting on the body (e.g., during braking, the vehicle decelerates while the body moves forward due to inertia, and thus the arrow points forward). The intensity of the red color reflected the magnitude of acceleration, with deeper red indicating stronger acceleration (see Figure 6).

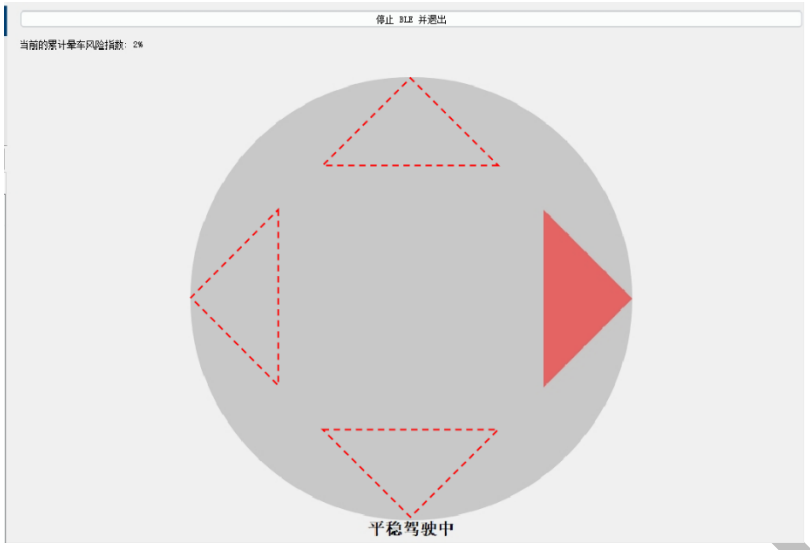

Figure 6. The informative interface providing the information on instantaneous acceleration.

3.3.3 Switch of the Interfaces

The three interfaces were mutually exclusive and dynamically changed based on the vehicle's acceleration. Drawing on previous research conducted by De Winkel et al. (2023), which established acceleration thresholds for different comfort levels (see Table 1), we defined two critical threshold values, corresponding to lower and upper acceleration limits, on both longitudinal and lateral directions.

The lower limit corresponded to an “excellent” level of comfort, while the upper threshold was dynamically adjusted based on MSI, as described in Table 2. Every minute, MSI was recalculated, and the corresponding MS risk level was used to update the upper limit in real time.

These two acceleration limits determined which interface was activated:

- If the current acceleration was below the lower limit, the encouragement interface was triggered (see Figure 4).
- If the acceleration exceeded the upper limit, the warning interface was displayed (see Figure 5).
- If the acceleration was between the lower and upper limits, the informative interface was activated (see Figure 6).

3.3. Experiment Design

A within-subject experiment design was adopted, involving two driver guidance conditions: one with our proposed feedback system and one without. Each participant pair (one driver and one passenger) completed two separate rides, corresponding to the two Driver guidance conditions. To minimize the potential influence of residual MS on the second ride, a minimum interval of five days was maintained between rides for the same participant pair. All rides were conducted in the same instrumented vehicle on a fixed 30-minute circular urban route. The route started at the Guangzhou campus of the Hong Kong University of Science and Technology, passing through Huangge Automobile City, and returning to the Guangzhou campus of the Hong Kong University of Science and Technology (see Figure 7). To reduce the impact of traffic variability on the results, all sessions were scheduled during non-rush hours, specifically, between 9:00 a.m. and 4:00 p.m. on weekdays.

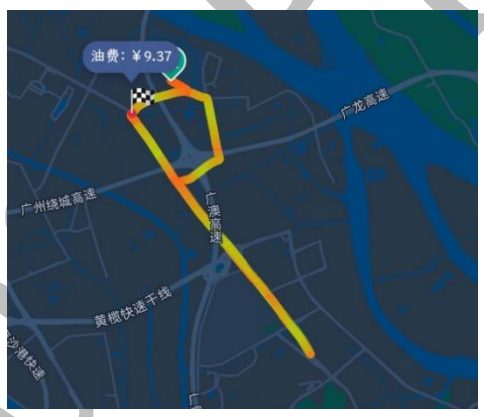

Figure 7. The predefined circular route for the ride.

To control potential gender-related effects, gender balance was maintained across the experiment. Four gender combinations were included: 1) male driver with male passenger, 2) male driver with female passenger, 3) female driver with male passenger, and 4) female driver with female passenger. Each combination consisted of four driver–passenger pairs, resulting in 16 pairs in total. The order of the experimental conditions (i.e., presence or absence of. the driver guidance system) was counterbalanced across pairs of participants to control for potential order effects (see Figure 8).

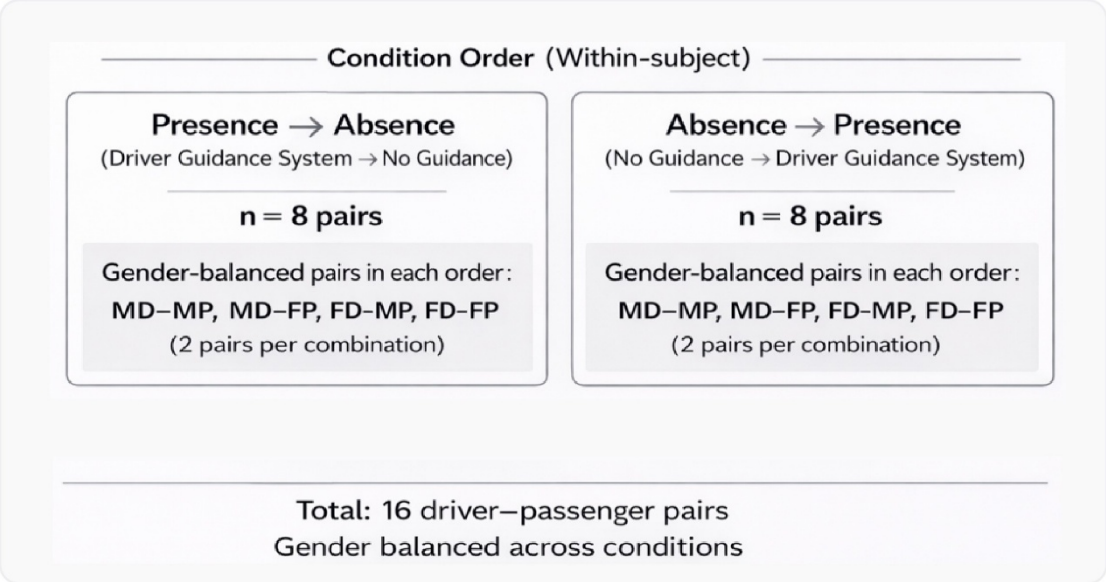

Figure 8. Counterbalanced order of experimental conditions; MD = male driver; MP = male passenger; FD = female driver; FP = female passenger.

3.6. Experiment Procedures

Following the guidelines Suwa et al. (2022), both driver and passenger participants were advised to maintain good health through self-care, have sufficient sleep the night before, and abstain from alcohol. Additionally, passenger participants were required to finish their meals at least one hour before the experiment.

Before each drive, the cabin environment was standardized across all trials, including wind speed, temperature, seat position and inclination, and audio narration levels. Upon the participants' arrival, all participants signed an informed consent outlining the study procedures, potential risks, and benefits.

In the briefing before the experiment, participants were provided only with general information regarding the study procedure and safety considerations. Passenger participants were not informed of the specific research hypotheses, the purpose of the driver guidance interface, nor the fact that drivers might adjust their driving behavior based on the interface. From the passenger’s perspective, the additional display was an auxiliary in-vehicle screen that visually changed during driving, without any explicit or

implicit emphasis on its experimental relevance. Moreover, passengers were not informed that MS was the primary objective of the study.

Before the start of each ride, passenger participants were introduced to the Chinese version of the Misery Scale (MISC; Lin and Guo (2022)), adapted from Bos et al. (2005), to assess MS levels (see Table 3). During the ride, they watched video clips on an in-vehicle display and reported their MS levels in MISC via their mobile phones every minute, as reminded by an auditory alert (90 dB, 1000 Hz, 1-second duration). To aid accurate reporting, a printed MISC explanation was provided near the video screen (see Fig. 2). To encourage the passenger participants to fully engage in the video-watching task so that the in-vehicle tasks were consistent across all drives, passenger participants were told that they would need to answer questions related to the video content after each ride. As a result, we found that video-watching performance did not differ between conditions (correctness rate: absence = 82.8%, SD = 21.8%; presence = 78.1%, SD = 20.2%; paired-samples t-test, p = .42). Furthermore, passenger participants were also specifically informed of their right to withdraw at any point, especially in cases of MS-induced nausea. If withdrawal occurred, the experiment would be stopped immediately at the nearest safe location to allow the participant to exit the vehicle.

Driver participants were instructed to drive as much mileage as possible within the 30-minute experiment session while maintaining passenger comfort as much as possible without compromising driving safety. To motivate drivers, drivers were informed that out of all participants, those who achieved the top 25% longest distance while also meeting the comfort criteria would receive an additional bonus. This incentive was designed to encourage drivers to maximize driving efficiency while balancing passenger comfort. Drivers were informed of the experimental route in advance, and no visual navigation system was used during the drive. Instead, route guidance and basic driving instructions (e.g., when to turn) were delivered via concise auditory prompts generated by the navigation system to avoid introducing additional

visual demands. Drivers were explicitly instructed that driving safety should always be the first priority, and drivers were not required to continuously monitor the guidance display. In addition, an experienced experimenter who was familiar with the route and traffic conditions sat in the front passenger seat throughout each session and was instructed to intervene or provide warnings if any safety concerns arose.

Each experimental session was concluded under one of the following conditions: the 30-minute time limit was reached, the passenger requested to stop, or the MISC score exceeded 7 ("Rather Nausea"), a commonly used termination threshold in previous MS research. However, no trial met the early termination criteria, and all sessions lasted 30 minutes. Driver participants were compensated at a rate of 100 Yuan per hour, and passenger participants at 60 Yuan per hour. Full compensation was granted to all participants after the data collection for the whole study was completed, regardless of their performance. This study was approved by the Human and Artefacts Research Ethics Committee of the Hong Kong University of Science and Technology (HSP-2024-0088).

Table 3. MISC for MS evaluation during the rides

Symptoms		MISC
No problems		0
Some discomfort, but no specific symptoms		1
Dizziness, cold/warm, headache, stomach/throat awareness, sweating, blurred vision, yawning, burping, tiredness, salivation,... but no nausea	Vague	2
	Little	3
	Rather	4
	Severe	5
Nausea	Little	6
	Rather	7
	Severe	8
	Retching	9
Vomiting		10

4. Data Analysis

4.1. Quantification of Vehicle Motion in a Ride

To compare the vehicle motions across Driver guidance conditions, the Motion Sickness Dose Values (MSDVs) were computed per the ISO2631-1 (1997) standard, which materializes the overall motion stimulus throughout a ride, following the formulation proposed by Yunus et al. (2021) and shown in Equation (9):

$$\boldsymbol{MSDV_{total}} = \sqrt{\boldsymbol{MSDV_x}^2 + \boldsymbol{MSDV_y}^2 + \boldsymbol{MSDV_z}^2} \quad (9)$$

In which, the component values, $MSDV_x$, $MSDV_y$, and $MSDV_z$, were derived through weighted integrations of acceleration signals along the lateral, longitudinal, and vertical axes, as described in Equations (10) and (11):

$$\boldsymbol{a_{i,w}(t)} = \boldsymbol{a_i(t)} \times \boldsymbol{W_i} \qquad \boldsymbol{i = x, y, z} \quad (10)$$

$$\boldsymbol{MSDV_i} = (\int_0^T (\boldsymbol{a_{i,w}(t)})^2)^{1/2} \quad (11)$$

In these equations, $\boldsymbol{W_i}$ denotes the frequency-dependent weighting factor applied to the acceleration in each respective direction. Specifically, ISO2631-1 (1997) guidelines were used to determine the vertical weighting for $MSDV_z$, while Donohew and Griffin (2004) provided the lateral and longitudinal frequency weightings for calculating $MSDV_x$ and $MSDV_y$.

4.2 Statistical Analysis

In this study, we used *R* 4.4.1 for statistical analysis following two steps:

Step 1: To test **H1**, we compared the motion-related driving performance, i.e., the riding distance and MSDV, between the driver guidance condition (i.e., *with* vs *without*), linear mixed-effects models were applied using the "lmer" function from the "lmerTest"

459 package (Kuznetsova et al., 2020). The driver–passenger pair was included as a random
460 effect to account for repeated measures. The model structures were as follows:

461 lmer(riding distance ~ condition + (1 | team))

462 lmer(MSDV ~ condition + (1 | team))

463 We conducted mixed-effects quantile regressions at the 25th, 50th, and 75th
464 quantile to further examine how vehicle acceleration (both lateral and longitudinal)
465 changed over time under different experimental conditions using the "lqmm" package
466 (Geraci, 2014) from R. Instead of using linear mixed-effects model, the quantile
467 regression provides more detailed information regarding the extreme accelerations,
468 which are more closely related to MS compared to average acceleration. The fixed
469 effects included time, experimental condition, and their two-way interaction, while the
470 dependent variables were the minute-by-minute mean absolute longitudinal and lateral
471 acceleration, respectively. These acceleration values were computed as the average over
472 the preceding one-minute interval, resulting in 30 data points for each participant in a
473 30-minute trial. The model structure was as follows:

474 lqmm(means of absolute longitudinal (or lateral) acceleration ~condition + time +
475 condition*time + (1 | team))

476 **Step 2:** To test **H2**, we explored if the driver guidance system influenced the
477 likelihood of passengers experiencing different levels of MS. We transformed the MISC
478 scores (ranging from 0 to 7) into binary outcomes (0 = no MS, 1 = MS) based on three
479 thresholds, i.e., MISC ≥ 2, MISC ≥ 4, and MISC ≥ 6, corresponding to "mild",
480 "moderate" and "severe" MS. If a participant's MISC score exceeded a given threshold,
481 they were labelled as experiencing a specific level of MS; otherwise, they were labelled
482 as experiencing a lower level of MS or no MS.

483 For each threshold, a mixed-effects logistic regression model was fitted using the
484 "glmmTMB" package (Bolker, 2019), again with the participant pair as a random effect.
485 To examine pairwise group differences, we used the "emmeans" package (Lenth et al.,

2024), applying the "Bonferroni correction" for multiple comparisons (Weisstein, 2004). The model structures were as follows:

glmmTMB(score ~ gender + condition + time + condition * time + (1 | team))

5. Results

5.1. The Motion-Related Driving Performance

As shown in Figure 9, no significant difference was found between the experimental conditions in terms of the driving distance ($p > .05$) or MSDV ($p > .05$).

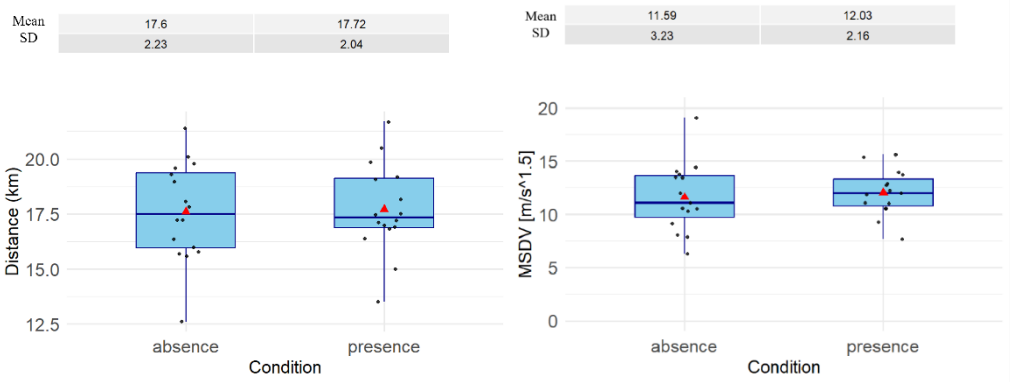

(a) (b)

Figure 9. Difference between the two experimental conditions: a) travelled distance; b) MSDV.

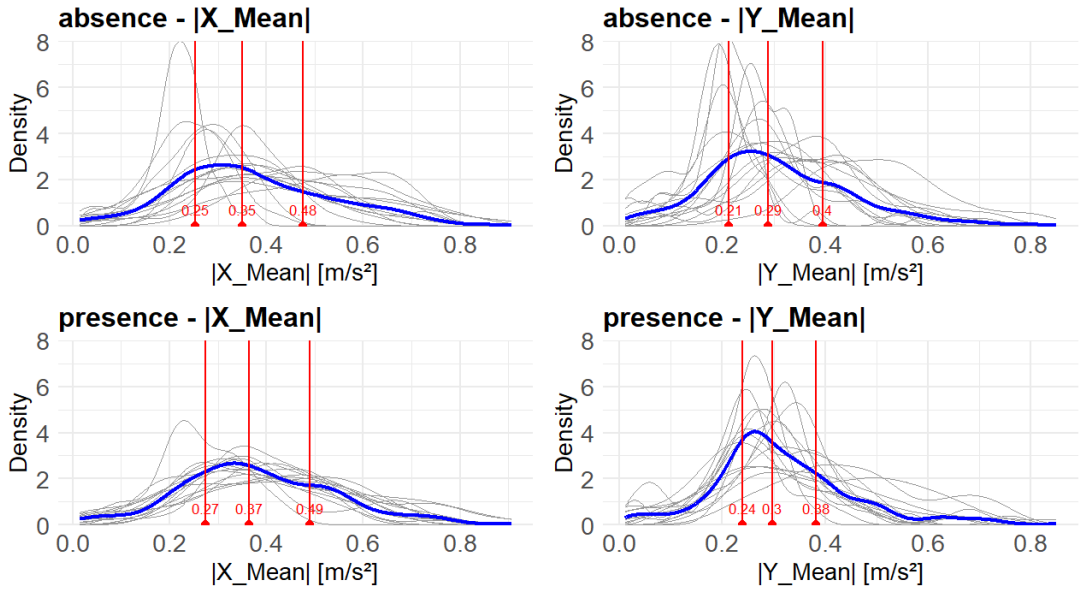

Figure 10. Probability-density plot. |X_Mean| represents the mean absolute longitudinal acceleration calculated per minute, while |Y_Mean| denotes the mean absolute lateral acceleration calculated per minute. The gray lines illustrate the distribution of mean absolute longitudinal (or lateral) acceleration for each participant, while the blue lines depict the distribution of mean absolute longitudinal (or lateral) acceleration for all participants within each experimental condition. From left to right, the vertical red lines indicate the 25th percentile, 50th percentile, and 75th percentile of the mean absolute longitudinal (and lateral) acceleration.

Figure 10 depicts the mean absolute longitudinal and lateral acceleration distributions for each experimental condition. The results of mixed-effect quantile regression for the mean absolute longitudinal acceleration as a dependent variable are summarized in Table 4. A significant interaction between time and experimental conditions was observed for all quantiles of the accelerations. Specifically, at the 25th percentile, the minute-to-minute change in absolute acceleration was, on average, approximately 0.002 m/s² lower with the interactive feedback system compared to the baseline (95% CI: –0.003, 0.000). Similar effects were observed at the 50th percentile (Δ = -0.002, 95% CI: –0.004, 0.000) and the 75th percentile (Δ = -0.002, 95% CI: –

0.003, 0.000). In other words, the introduction of the interactive feedback system has made the drivers more conservative with the progress of the experiment.

Table 4. Quantile regression results for the mean absolute longitudinal acceleration as a dependent variable; significant ($p < 0.05$) findings are bolded; CI: confidence interval

	25th Percentile		50th Percentile		75th Percentile	
	Estimate (SD)	95% CI	Estimate (SD)	95% CI	Estimate (SD)	95% CI
Intercept	**0.353 (0.025)**	**0.301, 0.403**	**0.353 (0.022)**	**0.310, 0.396**	**0.453 (0.021)**	**0.411, 0.495**
Condition	0.041 (0.024)	-0.005, 0.088	0.041 (0.020)	0.003, 0.080	**0.041 (0.021)**	**0.001, 0.082**
Time	0.001 (0.003)	-0.006, 0.008	0.001, 0.001	0.000, 0.003	0.001 (0.001)	-0.000, 0.003
Condition * time	**-0.002 (0.001)**	**-0.003, 0.000**	**-0.002, 0.001**	**-0.004, 0.000**	**-0.002 (0.001)**	**-0.003, 0.000**

The results of the mixed-effects quantile regression with the mean lateral acceleration as the dependent variable are summarized in Table 5. No significant main effect of the experimental condition, nor any interaction effect involving the experimental condition, was observed on lateral acceleration. However, it should be noted that a modest order effect was observed for lateral acceleration (i.e., the lateral acceleration was larger if the absence condition was the second trial of a participant, versus that if the absence condition was the first trial of a participant), whereas no such effect was observed for longitudinal acceleration. As discussed in Appendix A, the direction of this effect suggests a conservative bias rather than an inflation of the guidance effect.

Table 5. Quantile regression results for the mean absolute lateral acceleration as a dependent variable; significant ($p < 0.05$) findings are bolded

	25th Percentile		50th Percentile		75th Percentile	
	Estimate (SD)	95% CI	Estimate (SD)	95% CI	Estimate (SD)	95% CI
Intercept	**0.257 (0.017)**	**0.223, 0.291**	**0.257 (0.020)**	**0.217, 0.297**	**0.357 (0.022)**	**0.315, 0.399**
Condition	0.015 (0.015)	-0.014, 0.045	0.015 (0.012)	-0.009, 0.040	0.015 (0.015)	-0.014, 0.045
Time	**0.003 (0.001)**	**0.002, 0.004**	**0.003, 0.001**	**0.002, 0.004**	**0.003 (0.001)**	**0.002, 0.004**
Condition * time	-0.000 (0.001)	-0.003, 0.002	-0.000, 0.001	-0.002, 0.002	-0.000 (0.001)	-0.003, 0.002

5.2 Subjective MS Metrics

To further scrutinize the number of participants who experienced different levels of MS, Figure 11 further displays the number of participants experiencing MS, whose MISC scores exceeded the corresponding threshold and Table 6 summarizes the findings from three mixed-effect logistic regression models with MISC thresholds of 2 (Model 1), 4 (Model 2), and 6 (Model 3).

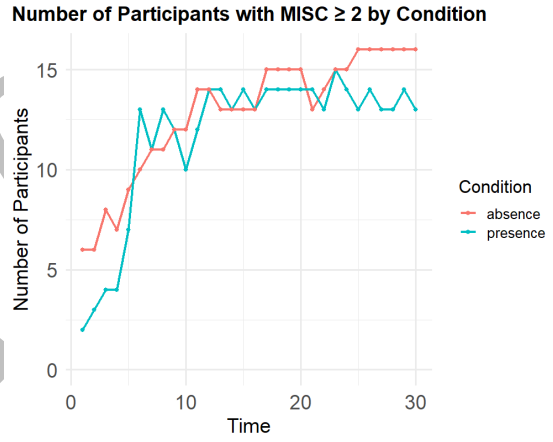

(a)

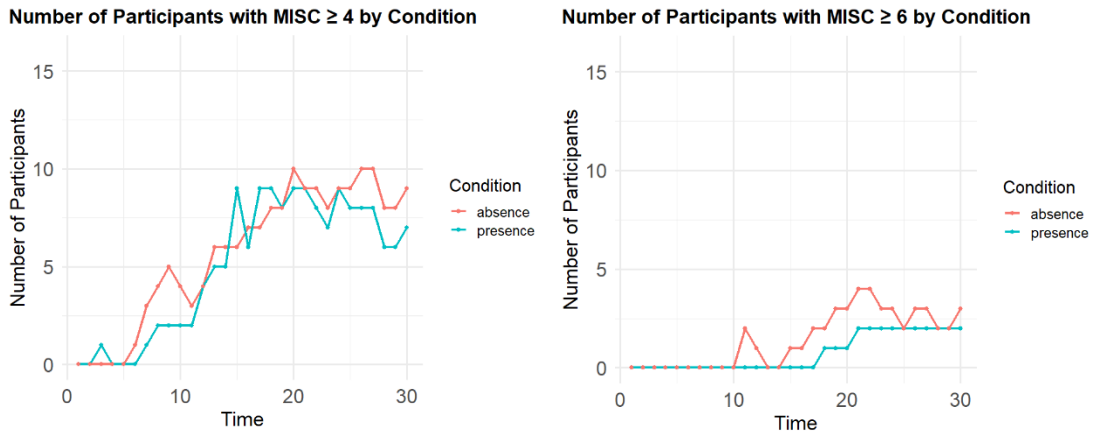

(b) (c)

542 Figure 11. Number of participants with MISC over the threshold

543

544 Table 6. Results of the mixed-effect logistic regression model

	Parameters	χ^2	DF	*p*-value
M1: Likelihood (MISC ≥ 2)	condition	0.08	1	.8
	time	96.61	1	**< .0001***
	gender	0.05	1	.8
	condition*time	9.57	1	**.002***
M2: Likelihood (MISC ≥ 4)	condition	0.09	1	**.**8
	time	104.21	1	**< .0001***
	gender	0.18	1	.7
	condition*time	0.48	1	.5
M3: Likelihood (MISC ≥ 6)	condition	3.55	1	.06
	time	33.98	1	**< .0001***
	gender	0.17	1	.7
	condition*time	0.88	1	.3

545 Note: * indicates statistical significance, and *DF* denotes degrees of freedom.

546

547 As shown in Table 6, only the interaction between the experimental condition and
548 time in the M1 model was found to be significant. Specifically, the time effect was
549 significantly greater when no driver guidance system was provided than when such a
550 system was provided, with an odds ratio (OR) of 1.11, 95% confidence interval
551 (95%CI): [1.04, 1.18], $\chi^2(1) = 9.49$, $p = 0.002$. In other words, with each additional
552 minute, the odds of experiencing slight or higher MS (MISC ≥ 2) increased
553 approximately 11% faster when the driver guidance system was not provided as

compared to when such a system was provided (see Figure 12). Importantly, supplementary analyses showed that the experiment order did not affect MS, suggesting that the reported interaction effects between condition and time were not confounded by any carry-over effects (see Appendix A).

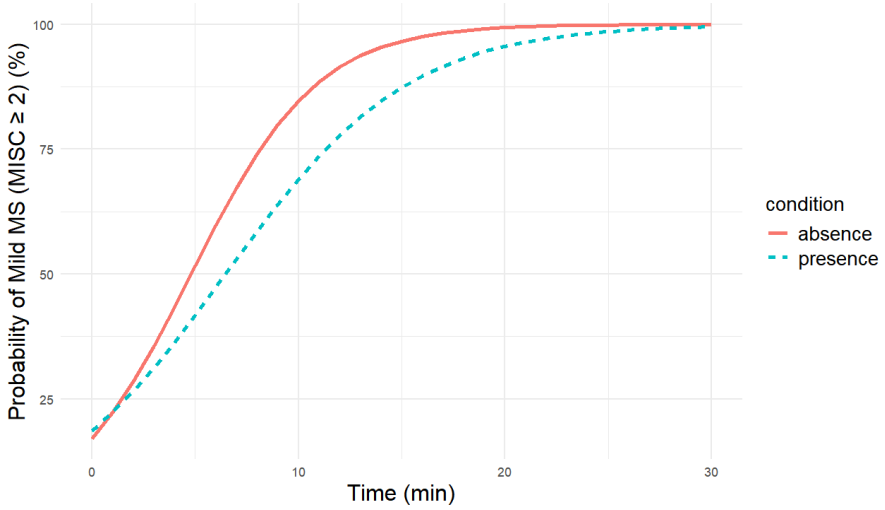

Figure 12. Likelihood of experiencing mild or more severe MS over time

6. Discussion

In this study, we designed and evaluated an interactive driver guidance system to promote a less aggressive and thus more MS-friendly driving style. We hypothesized that with such a system, the vehicle dynamics would be smoother (H2) and passengers would experience a lower level of MS (H2). Our findings support these hypotheses.

6.1. Interface design considerations

It should be noted that our design of the driver guidance interface intentionally conveyed motion-sickness-related risk information using non-semantic visual features such as color intensity and motion direction, which can be efficiently perceived through peripheral vision without requiring explicit semantic interpretation through focal vision and minimizing interference with driving tasks.

Further, the driver guidance interface in this study was intentionally designed as an information-level feedback system (i.e., what has happened) rather than an action-oriented one (i.e., what the drivers should do, such as “brake more gently” or “turn more

smoothly"). This is because the action-oriented instructions may not always be contextually appropriate in real-world driving and could potentially conflict with drivers' immediate safety judgments. By providing information related to motion sickness risk rather than explicit commands, the current design aims to support driver awareness while preserving driver autonomy in determining how to adapt driving behavior under varying traffic conditions, which may help them build up a connection between what they do and what the passengers might feel, and thus enable internalization of a more MS-friendly driving style over time.

6.2. The effect of driver guidance on MS

Although no significant differences were observed in the likelihood of experiencing moderate (MISC $\geq$ 4) or severe (MISC $\geq$ 6) symptoms; our driver guidance system has successfully reduced the chance of passenger experiencing mild or higher MS (MISC $\geq$ 2), suggesting a delayed onset of or a reduced likelihood of mild MS symptoms with the driver guidance system. However, more severe MS might be related to more than the driving style, but also the characteristics of the passengers (such as the susceptibility, Turner (1999)); the design of the vehicle cabin (Salter et al., 2019), or the dynamics of the chess (DiZio et al., 2018), which can hardly be mitigated by the driving style alone. It is also possible that in the experiment, the passenger comfort was framed to be associated with an additional bonus they could obtain. Thus, drivers might be attentive to passenger comfort and maintain relatively smooth driving, resulting in the low incidence of moderate (321 out of 960 records) and severe (61 out of 960 records) MS reports. This diminished the observable impact of the driver guidance system on more severe MS.

6.3. Vehicle dynamics and driving style

Although we did not find significant differences between the groups with and without the driver guidance system in terms of the travelled distance and MSDV, the driver guidance system has led to a smaller longitudinal acceleration with the progress

601 of the drive. Specifically, with the driver guidance system, the mean absolute
602 longitudinal accelerations tended to increase more slowly over time compared to those
603 without such a guidance condition. This aligns with our expectations (H1) and the MS
604 mitigation effect of the driver guidance system observed in our study. It is likely that
605 early in a drive, when passengers had not yet experienced MS, the warning threshold
606 of the system was relatively high (see Table 2). Thus, drivers had more freedom to drive
607 more aggressively. As the ride progressed, passengers gradually became more likely to
608 experience MS, and thus the threshold of the system warning would become lower (in
609 other words, the warning interfaces are more likely to be triggered). This encouraged
610 drivers to adopt smoother and more conservative driving behaviors to avoid triggering
611 warnings. In contrast, drivers in the no-feedback condition lacked such real-time
612 feedback and had to rely solely on their own perception to balance distance
613 maximization and passenger comfort. This may have led to more aggressive behavior
614 among the drivers without the guidance in the later stage of the drive as compared to
615 drivers who were provided with the guidance system.

616 This also explains the non-significant differences in MSDV and total distance. It is
617 likely that drivers in both conditions were incentivized to maximize travel distance.
618 Thus, they have tried to balance the smoothness of the drive and the driving efficiency.
619 As a result, instead of driving slower in general, they would prefer slight accelerations
620 and avoid abrupt accelerations. This strategy would not affect MSDV, as it is an integral
621 of acceleration, but would lead to fewer MS-inducing accelerations. Thus, our proposed
622 guidance system can enhance driver awareness of passenger comfort and help maintain
623 a better balance between driving efficiency and riding quality.

624 ## 7. Limitations

625 Several limitations of this study should be pointed out. First, our focus on “risky”
626 drivers and “highly susceptible” passengers may limit the generalizability of the
627 findings. Exploring a wider range of driver profiles and heterogeneous passengers is a

necessary step to further validate our proposed system. Second, the urban route used in the experiment, though representative of everyday driving, restricted the variations in speed and acceleration in a trip. Future studies could include highway driving or more diverse routes to better evaluate the effectiveness of our system in more diverse traffic scenarios. Third, this study was conducted using a fuel-powered vehicle. Previous research suggests that electric vehicles (EVs), due to their more abrupt dynamic responses, may induce more severe MS (Xie et al., 2024). Future research should validate the effectiveness of our proposed system in EVs. Fourth, the feedback thresholds in this study were based on prior comfort research and were not dynamically tailored to individual driving styles, nor the real-time MS level of the passengers. An adaptive system that considers driver behavior, passenger states, and road conditions could potentially yield better MS mitigation effects. In addition, drivers with different personalities may have different levels of acceptance of the suggestions from the feedback system (Marafie et al., 2021), and they may expect different ways of information framing (Marafie et al., 2021). Future research may consider an adaptive feedback system to improve the compliance rate of the MS mitigation suggestions. Finally, the current interface design focuses on information-level feedback and therefore requires drivers to interpret the visual cues and translate them into appropriate control actions. This additional transformation step may reduce immediate intuitiveness and increase cognitive demands, particularly for less experienced drivers. While this conservative design was chosen to minimize interference with the primary driving task in this initial exploration, future work could investigate more action-oriented or hybrid feedback designs that more directly link system feedback to driving actions while maintaining safety and usability. Future research should also include a baseline condition with a provided interface but without meaningful information to avoid biasing passengers' responses to MS-related questionnaires.

8. Conclusions

As the first known study to mitigate MS through driver behavior guidance, our research showed promising results for alleviating MS. In an on-road study, we validated the effectiveness of our proposed driver guidance system in mitigating MS while maintaining travel efficiency. In real-world contexts, the MS has been widely reported and complained about in short commutes or rideshare services (Broadwater, 2023). Thus, even a modest delay in the onset of passenger discomfort can significantly enhance the travel experience. This is particularly relevant in rideshare scenarios, where drivers often prioritize efficiency at the expense of passenger comfort, aiming to deliver passengers to their destinations as quickly as possible in order to maximize their income. Our system offers a potential solution by helping drivers be aware of the passenger comfort while maintaining high efficiency, which may significantly improve the service quality by making a better trade-off between efficiency and passenger well-being.

Declaration of Competing Interest

The authors acknowledge that they have no conflicts of interest in this work.

Acknowledgments

This research is supported by the Guangzhou-HKUST(GZ) Joint Funding Scheme (No. 2023A03J0150), and the Guangdong Provincial Key Lab of Integrated Communication, Sensing and Computation for Ubiquitous Internet of Things (No.2023B1212010007).

REFERENCES

Aarti, D. (2025). *Smart vehicle cabin market research report*. MarketResearchFuture. Retrieved February from https://www.marketresearchfuture.com/reports/smart-vehicle-cabin-market-30964

Barth, M., & Boriboonsomsin, K. (2009). Energy and emissions impacts of a freeway-based dynamic eco-driving system. *Transportation Research Part D: Transport and Environment*, *14*(6), 400-410.

Bolker, B. (2019). Getting started with the glmmTMB package. *Cran. R-project vignette*, *9*.

Bos, J., & Bles, W. (1998). Modelling motion sickness and subjective vertical mismatch detailed for vertical motions. *Brain research bulletin*, *47*(5), 537-542.

Bos, J. E., MacKinnon, S. N., & Patterson, A. (2005). Motion sickness symptoms in a ship motion simulator: effects of inside, outside, and no view. *Aviation, space, and environmental medicine*, *76*(12), 1111-1118.

Brietzke, A., Xuan, R. P., Dettmann, A., & Bullinger, A. C. (2021). Influence of dynamic stimulation, visual perception and individual susceptibility to car sickness during controlled stop-and-go driving. *Forschung im Ingenieurwesen-Engineering Research*, *85*(2), 517-526.

Broadwater, A. (2023). *So that's why you feel carsick In Ubers and Cabs*. HUFFPOST. Retrieved April from https://www.huffpost.com/entry/nauseous-uber-lyft-cab_l_649310c8e4b0aec6b7fdc34c

Buchheit, B., Schneider, E. N., Alayan, M., Dauth, F., & Strauss, D. J. (2021). Motion sickness prediction in self-driving cars using the 6DOF-SVC model. *IEEE Transactions on Intelligent Transportation Systems*, *23*(8), 13582-13591.

De Winkel, K. N., Irmak, T., Happee, R., & Shyrokau, B. (2023). Standards for passenger comfort in automated vehicles: Acceleration and jerk. *Applied Ergonomics*, *106*, 103881.

DiZio, P., Ekchian, J., Kaplan, J., Ventura, J., Graves, W., Giovanardi, M., Anderson, Z., & Lackner, J. R. (2018). An active suspension system for mitigating motion sickness and enabling reading in a car. *Aerospace medicine and human performance*, *89*(9), 822-829.

Donohew, B. E., & Griffin, M. J. (2004). Motion sickness: effect of the frequency of lateral oscillation. *Aviation, space, and environmental medicine*, *75*(8), 649-656.

Geraci, M. (2014). Linear quantile mixed models: the lqmm package for Laplace quantile regression. *Journal of Statistical Software*, *57*, 1-29.

Golding, J. F. (2006). Predicting individual differences in motion sickness susceptibility by questionnaire. *Personality and Individual differences*, *41*(2), 237-248.

Htike, Z., Papaioannou, G., Siampis, E., Velenis, E., & Longo, S. (2020). Motion sickness minimisation in autonomous vehicles using optimal control. International Conference on Robotics in Alpe-Adria Danube Region,

Irmak, T., Kotian, V., Happee, R., de Winkel, K. N., & Pool, D. M. (2022). Amplitude and temporal dynamics of motion sickness. *Frontiers in Systems Neuroscience*, *16*, 866503.

ISO2631-1. (1997). Mechanical vibration and shock: Evaluation of human exposure to whole-body vibration—Part 1: General requirements (ISO Standard No. 2631-1). In: International Organization for Standardization.

ISO8855. (2011). Road vehicles—Vehicle dynamics and road-holding ability—Vocabulary (ISO Standard No. 8855:2011). In: International Organization for Standardization.

Kamiji, N., Kurata, Y., Wada, T., & Doi, S. i. (2007). Modeling and validation of carsickness mechanism. SICE Annual Conference 2007,

Karjanto, J., Wils, H., Yusof, N. M., Terken, J., Delbressine, F., & Rauterberg, M. (2022). Measuring the perception of comfort in acceleration variation using electrocardiogram and self-rating measurement for the passengers of the automated vehicle. *Journal of Engineering Science and Technology*, *17*(1), 180-196.

Karjanto, J., Yusof, N. M., Wang, C., Terken, J., Delbressine, F., & Rauterberg, M. (2018). The effect of peripheral visual feedforward system in enhancing situation awareness and mitigating motion sickness in fully automated driving. *Transportation research part F: traffic psychology and behaviour*, *58*, 678-692.

Kuznetsova, A., Brockhoff, P. B., Christensen, R. H. B., & Jensen, S. P. (2020). *lmerTest: Tests in linear mixed effects models*. In https://cran.r-project.org/web/packages/lmerTest/index.html

Lenth, R., Bolker, B., Buerkner, P., Giné-Vázquez, I., Herve, M., Jung, M., Love, J., Miguez, F., Piaskowski, J., Riebl, H., & Singmann, H. (2024). *Estimated marginal means, aka least-squares means*. In https://cran.r-project.org/web/packages/emmeans/

Li, D., Tang, B., Yu, T., Chen, L., Zhou, K., Qie, N., Shi, Y., Lu, C., & Zhang, H. (2024). Can we use smart phone on a moving vehicle without worrying about carsickness? developing an effective motion cue APP with driving simulator and real vehicle experiments. *International Journal of Human–Computer Interaction*, 1-15.

Li, D., Xu, B., Chen, L., Tang, B., Yu, T., Zhou, K., Qie, N., Shi, Y., Lu, C., & Zhang, H. (2023). Mosi app-a motion cueing application to mitigate car sickness while performing non-driving task. International Conference on Human-Computer Interaction,

Lin, Y., & Guo, G. (2022). *Research on the evaluation and relief with olfaction method of passengers carsickness degree* [master's thesis, Chongqing University].

Maculewicz, J., Larsson, P., & Fagerlönn, J. (2021). Intuitive and subtle motion-anticipatory auditory cues reduce motion sickness in self-driving cars. *International journal of human factors and ergonomics*, *8*(4), 370-392.

Marafie, Z., Lin, K.-J., Wang, D., Lyu, H., Liu, Y., Meng, Y., & Ma, J. (2021). AutoCoach: an intelligent driver behavior feedback agent with personality-based driver models. *Electronics*, *10*(11), 1361.

Miksch, M., Steiner, M., Miksch, M., & Meschtscherjakov, A. (2016). Motion sickness prevention system (MSPS) reading between the lines. Adjunct

Proceedings of the 8th International Conference on Automotive User Interfaces and Interactive Vehicular Applications,

Paganelli, S., Yunus, I., & Fagiano, L. (2022). Comfort-Aware Trajectory Planning in Autonomous Driving via Multi-Objective Nonlinear Model Predictive Control. 2022 IEEE Conference on Control Technology and Applications (CCTA),

Reason, J. (1975). Motion sickness. In: Academic Press.

Riccio, G. E., & Stoffregen, T. A. (1991). An ecological theory of motion sickness and postural instability. *Ecological psychology*, *3*(3), 195-240.

Salter, S., Diels, C., Herriotts, P., Kanarachos, S., & Thake, D. (2019). Motion sickness in automated vehicles with forward and rearward facing seating orientations. *Applied Ergonomics*, *78*, 54-61.

Siddiqi, M. R., Milani, S., Jazar, R. N., & Marzbani, H. (2022). Motion sickness mitigating algorithms and control strategy for autonomous vehicles. *IEEE Transactions on Intelligent Transportation Systems*, *24*(1), 304-315.

Smyth, J., Birrell, S., Woodman, R., & Jennings, P. (2021). Exploring the utility of EDA and skin temperature as individual physiological correlates of motion sickness. *Applied Ergonomics*, *92*, 103315.

Smyth, J., Robinson, J., Burridge, R., Jennings, P., & Woodman, R. (2021). Towards the management and mitigation of motion sickness–an update to the field. Congress of the International Ergonomics Association,

Sun, L., Yang, C., & Chang, R.-s. (2014). Revision and preliminary application of multidimensional driving style scale. *Ergonomics*, *20*(2), 4.

Suwa, T., Sato, Y., & Wada, T. (2022). Reducing motion sickness when reading with head-mounted displays by using see-through background images. *Frontiers in Virtual Reality*, *3*, 910434.

Turner, M. (1999). Motion sickness in public road transport: passenger behaviour and susceptibility. *Ergonomics*, *42*(3), 444-461.

Turner, M., & Griffin, M. J. (1999). Motion sickness in public road transport: the effect of driver, route and vehicle. *Ergonomics*, *42*(12), 1646-1664.

Vaezipour, A., Rakotonirainy, A., & Haworth, N. (2015). Reviewing in-vehicle systems to improve fuel efficiency and road safety. *Procedia Manufacturing*, *3*, 3192-3199.

Vaezipour, A., Rakotonirainy, A., Haworth, N., & Delhomme, P. (2018). A simulator evaluation of in-vehicle human machine interfaces for eco-safe driving. *Transportation research part A: policy and practice*, *118*, 696-713.

Vaiana, R., Iuele, T., Astarita, V., Caruso, M. V., Tassitani, A., Zaffino, C., & Giofrè, V. P. (2014). Driving behavior and traffic safety: an acceleration-based safety evaluation procedure for smartphones. *Modern Applied Science*, *8*(1), 88.

Wada, T., & Yoshida, K. (2016). Effect of passengers' active head tilt and opening/closure of eyes on motion sickness in lateral acceleration environment of cars. *Ergonomics*, *59*(8), 1050-1059.

Weisstein, E. W. (2004). *Bonferroni correction*. Wolfram Mathworld. https://mathworld.wolfram.com/

Xie, W., Huang, C., Yan, S., & He, D. (2024). Do electric vehicles induce more motion sickness than fuel vehicles? A survey study in China. Transport Research Board, Washington, U.S.

Xu, Q., Fu, R., Wu, F., Wang, B., & Chen, T. (2023). A speed limit advisory system provided by in-vehicle HMI considering auditory perception characteristics for connected environment. *Transportation research part F: traffic psychology and behaviour*, *92*, 353-368.

Yunus, I., Jerrelind, J., & Drugge, L. (2021). Evaluation of motion sickness prediction models for autonomous driving. The IAVSD International Symposium on Dynamics of Vehicles on Roads and Tracks,

Appendix A. Carry-over analyses

A.1 Vehicle motion

To examine potential carry-over effects in driving behavior, we fitted quantile mixed-effects models using the data from the guidance absence condition, with the mean absolute longitudinal or lateral acceleration as the dependent variable. These acceleration values were computed by averaging over consecutive one-minute intervals, yielding 30 observations per participant within each 30-minute trial. The model structure was as follows:

lqmm(means of absolute longitudinal (or lateral) acceleration ~order of guidance absence + time + (1 | team))

For longitudinal acceleration, the order of the guidance absence condition (i.e., whether the condition appeared in the first or second trial of a participant) was not statistically significant at the 25th, 50th, or 75th percentiles, as all corresponding 95% confidence intervals included zero (Table A-1). This indicates no detectable carry-over effect in longitudinal vehicle dynamics.

For lateral acceleration, the order of guidance absence exhibited a small but statistically significant effect across all examined quantiles (Table A-2), with lower lateral acceleration values when the guidance absence condition occurred in the second trial than in the first trial. This pattern indicates that a smoother driving style, as a result of the guidance, persisted into the subsequent guidance absence trial. However, such a carry-over effect would be expected to attenuate differences between the guidance presence and guidance absence conditions, thereby yielding a conservative estimate of the guidance system's effect rather than inflating it.

Table A-1. Quantile regression results for the mean absolute longitudinal acceleration as a dependent variable; significant ($p < 0.05$) findings are bolded; CI: confidence interval

	25th Percentile		50th Percentile		75th Percentile	
	Estimate (SD)	95% CI	Estimate (SD)	95% CI	Estimate (SD)	95% CI
Order of guidance absence	-0.059 (0.040)	-0.138, 0.019	-0.059 (0.045)	-0.147, 0.029	-0.059 (0.047)	-0.150, 0.032
Time	**0.003 (0.001)**	**0.002, 0.005**	**0.003, 0.001**	**0.002, 0.004**	**0.003 (0.001)**	**0.002, 0.004**

Table A-2. Quantile regression results for the mean absolute lateral acceleration as a dependent variable; significant ($p < 0.05$) findings are bolded; CI: confidence interval

	25th Percentile		50th Percentile		75th Percentile	
	Estimate (SD)	95% CI	Estimate (SD)	95% CI	Estimate (SD)	95% CI
Order of guidance absence	**-0.087 (0.029)**	**-0.143, -0.031**	**-0.087 (0.032)**	**-0.149, -0.024**	**-0.087 (0.033)**	**-0.152, -0.021**
Time	0.001 (0.003)	-0.004, 0.006	0.001, 0.001	-0.000, 0.003	0.001 (0.001)	-0.000, 0.003

A.2 Motion sickness

To assess whether a similar carry-over effect was present at the level of passenger outcomes, we conducted mixed-effects logistic regression analyses using the data from the guidance absence condition, with motion sickness as the dependent variable:

glmmTMB(score ~ order of guidance absence + time + (1 | team))

Across all three severity thresholds (MISC ≥ 2, ≥ 4, and ≥ 6), the order of the guidance absence condition was nonsignificant, whereas time showed the expected strong effect (Table A-3). These results indicate that, although a modest learning-related

carry-over effect was observed in lateral vehicle acceleration, it did not translate into a difference in passengers' reported motion sickness.

Table A-3. Results of the mixed-effect logistic regression model

	Parameters	χ^2	DF	p-value
M1 (MISC ⩾ 2)	Order of guidance absence	0.005	1	.9
	Time	**52.68**	**1**	**< .0001***
M2 (MISC ⩾ 4)	Order of guidance absence	2.68	1	.1
	Time	**76.06**	**1**	**< .0001***
M3 (MISC ⩾ 6)	Order of guidance absence	2.33	1	.1
	Time	**29.28**	**1**	**< .0001***

Taken together, these supplementary analyses suggest that the order-related carry-over effects were either negligible (longitudinal acceleration and motion sickness) or modest and conservative in nature (lateral acceleration). In other words, any such carry-over would be expected to reduce, rather than exaggerate, differences between the guidance presence and guidance absence conditions. Therefore, the reported effects of the guidance system can be interpreted as robust and conservative.

Weiyin Xie received a BSc and MSc from the University of Duisburg-Essen, and a PhD from the Hong Kong University of Science and Technology (Guangzhou). He is currently a Lecturer at the Guangzhou Maritime University.

Haolong Hu received a BEng from Jinan University and an MPhil from the Hong Kong University of Science and Technology (Guangzhou). He is currently an Emerging Talent Program Trainee at HSBC.

Dengbo He received an M.S. degree from Shanghai Jiao Tong University in 2016 and a PhD degree from the University of Toronto in 2020. He is currently an Assistant Professor at the Thrust of Intelligent Transportation, the Hong Kong University of Science and Technology (Guangzhou).